https://doi.org/10.5194/egusphere-2025-3867
Preprint. Discussion started: 15 August 2025

Cold spells induced by slow and amplified atmospheric waves

Morteza Babaei[1*], Rune Grand Graversen[1,2], Johannes Patrick Stoll[2], and Jakub Petříček[1]

[1]Department of Physics and Technology, University of Tromsø, Tromsø, Norway
[2]Norwegian Meteorological Institute, Tromsø, Norway

Correspondence: Morteza Babaei (morteza.babaei@uit.no)

Abstract. Cold spells in the Northern Hemisphere mid-latitudes have been linked to planetary waves. Yet the mechanisms by which these waves impact cold-spell formation remain unclear. Here we develop novel metrics to separately measure the amplitude and speed of ridges and troughs, examining the behavior of planetary waves during winter cold spells. Our findings indicate that while the planetary waves across the entire mid-latitudes experience significant changes during cold spells, local wave dynamics play a major role in developing these events. The nearest upstream ridge and downstream trough of the cold-spell region are located in a way that facilitates development of the extreme cold anomaly. This ridge and trough amplify and slow, enhancing and prolonging southward advection of cold air from the Arctic into the cold-spell region. The slow and amplified upstream ridge and downstream trough occur several days before the region's minimum temperature, suggesting these local wave anomalies induce cold-spell formation.

1 Introduction

The large-scale mid-latitude waves play a crucial role in shaping weather patterns in the mid-latitudes (Holton and Hakim, 2013). In 1937, Bjerknes provided pioneering work on a dynamical explanation for the movement of mid-latitude waves (Bjerknes, 1937). His elucidation on the movement of zonal pressure disturbances inspired Rossby to provide a mathematical description of the atmosphere's planetary wave behavior, which we now refer to as Rossby waves (Rossby et al., 1939). Rossby waves are large-scale atmospheric phenomena characterized by meandering patterns in winds, primarily influenced by pressure differences and the Earth's rotation and the resulting variation of the Coriolis effect with latitude (Holton and Hakim, 2013). Slow-moving (quasi-stationary) Rossby waves can be associated with strong waveguide occurrences (White and Mareshet, 2025) and atmospheric blocking (Namias and Clapp, 1944; Berggren et al., 1949; Riboldi et al., 2020).

The ability of high-amplitude quasi-stationary Rossby waves to generate extreme weather events has been acknowledged (e.g., Hoskins and Woollings, 2015; White et al., 2022). An increase in meridional amplitude of Rossby waves may enhance the meridional exchange of warm and cold air, leading to the advection of cold air further to the south and warm air to the north (Zschenderlein et al., 2018; Jolly et al., 2021). Slow movement of Rossby waves may lead to weather persistence, enhancing the probability of development of extreme weather events, such as floods, droughts, heat waves, and cold spells (Francis and Vavrus, 2012; Pfleiderer and Coumou, 2018; Riboldi et al., 2020; Wicker et al., 2024). A negatively tilted trough, extending from northwest to southeast up through the troposphere, generated through strengthening the wind shear, is another type of

https://doi.org/10.5194/egusphere-2025-3867
Preprint. Discussion started: 15 August 2025

atmospheric wave that may generate circumstances favorable for severe weather (Macdonald, 1976). Therefore, to understand the formation of extreme weather, it is critical to take the dynamics of Rossby waves into account.

The frequency of extreme events has risen in recent decades due to anthropogenic warming (IPCC; Seneviratne et al., 2021), and they are likely to become more intense and break the previous extreme records by a large margin in the following decades (Fischer et al., 2021). One such recent catastrophe is the late October 2024 flash floods in Spain, which caused 224 fatalities and substantial economic damage (WMO, 2024; Suardy, 2024). In 2024, 27 extreme weather events, including two winter storm events, each with losses exceeding one billion dollars, affect the United States. On top of the significant economic damage of these events, they caused the deaths of 568 people (NOAA, 2025). In addition, despite the warming Earth, cold spells and heavy snowfalls across the Northern Hemisphere have increased (e.g., Cohen et al., 2021; Overland et al., 2021; Cohen et al., 2024). On January 13, 2024, Billings, Montana, recorded its lowest temperature ever measured (Cassidy, 2024), during the warmest winter ever recorded in the continental United States (NOAA, 2024). Such unusually low temperatures also occur in Scandinavia recently. On January 3, 2024, the Swedish village of Kvikkjokk recorded Sweden's lowest January temperature in 25 years (Doermann, 2024).

It has been suggested that the increases in severe events, specifically cold spells, are linked to Arctic amplification (AA), a phenomenon by which the Arctic warms faster than the mid-latitudes (e.g., Francis and Vavrus, 2012; Cohen et al., 2014): the AA is weakening the jet stream, making the large-scale atmospheric waves more wavy (Francis and Vavrus, 2012; Coumou et al., 2015; Stendel et al., 2021). In addition, Rossby waves become more stationary, resulting in an increase in the frequency of extreme weather(Francis and Vavrus, 2012). This hypothesis, however, has been questioned by several studies (e.g., Barnes, 2013; Screen and Simmonds, 2013; Blackport et al., 2022, 2024).

A recent study shows heat waves in some regions are associated with slow waves, whereas in other regions with fast waves (Wicker et al., 2024). In addition, it is argued high propagation speeds of atmospheric blocking, identified using a blocking cell-tracking algorithm, can lead to significant surface temperature anomalies (van Mourik et al., 2025). These findings emphasize inconsistency in our understanding of the role of large-scale circulation in mid-latitude extreme events across different regions. Here, we attempt to analyze the large-scale structure of Rossby waves during cold spells. Cold spells are particularly of interest in the context of Rossby waves because these cold extremes are argued to be primarily driven by the large-scale advection of cold air from higher latitudes (Tuel and Martius, 2024). Hence, this study further investigates the role of Rossby waves in causing cold spells.

2 Methods

In this study, we used the European Centre for Medium-Range Weather Forecasts (ECMWF) analysis 5th Generation (ERA5) dataset with a horizontal resolution of 0.25°×0.25° (Hersbach et al., 2020) for the period 1978-2024. The study is for the winter season (December-January-February) and the satellite era. Minimum daily temperature and daily average temperature are obtained based on hourly ERA5 data. Additionally, 3-hourly geopotential height data at 300 hPa, 500 hPa, and 850 hPa are utilized.

https://doi.org/10.5194/egusphere-2025-3867
Preprint. Discussion started: 15 August 2025

2.1 Study regions selection

It may appear attractive to adopt the climate reference regions suggested by the IPCC (Iturbide et al., 2020) to align the boundaries of our study regions. However, cold spells manifest spatially differently than do the seasonal mean temperature patterns used in identifying the IPCC climate reference regions. For instance, in January 2024, cold spells occurred in Scandinavia, while there were no such events in the British Isles (Doermann, 2024). The IPCC classifies all these countries in a single region, while in our study they are classified in two regions. In addition, the interest here is to select regions in which cold spells are assumed to be originating from the Arctic cold air. To select the regions for the study on cold spells, areas with the largest cold anomaly contribution to the historical extreme cold days on the hemispheric scale are chosen (see the supplementary information). The regions include Northwest Canada (R01), Northwest US and Southwest Canada (R02), Central US (R03), British Isles (R04), Scandinavia (R05), Europe (R06), Northwest Russia (R07), Southwest Russia (R08), and Northern Siberia (R09).

2.2 Cold spells

To identify cold spells and their magnitudes, the cold wave magnitude index daily (CWMId; Morlot et al., 2023) is applied at each horizontal grid point. The daily cold spells index is based on at least three consecutive days below a daily threshold, defined as the 90th percentile of anomalies relative to the climatology of minimum daily air temperature smoothed with a 31-day running mean filter. The climatology is based on the reference period 1981–2020. The background trend is small relative to the daily anomalies and we have checked that it does not affect the overall conclusions drawn in the paper (not shown). If 50 % or more of the grid points within each region experience cold spells on a given day, it is considered a cold spell day in that region. Applying grid-point thresholds between 20 percent and 70 percent are also tested to ensure that the drawn overall conclusions remain unchanged for an altered threshold.

2.3 Wave speed

In order to investigate the role of planetary-scale waves, a Fourier decomposition of geopotential height (gph) is employed to separate the field into distinct harmonic waves based on the zonal wave number. The combination of the first five waves is regarded as an estimation of planetary-scale waves (Z1–5; solid line in Fig. 1a). We estimate the speed of planetary wave zonal propagation by utilizing a top-ridge and bottom-trough tracking algorithm (Fig. 1a). Small amplitude ridges and troughs are ignored since they are often short lived (red stars in Fig. 1a). This is accomplished by considering a threshold for the gph at each local maximum (ridge) and local minimum (trough): At each time step (3-hourly) and latitude, the gph at the ridge (trough) position must be greater (less) than the gph of 30 degrees to the west and east of the ridge (trough) position plus (minus) 8% of the Z1–5 amplitude (see blue texts and arrows in Fig. 1a). The Z1–5 amplitude is defined as the difference between the highest ridge and the lowest trough at all longitudes around a latitude circle at each time step and latitude. These criteria were carefully chosen after multiple experiments to ensure that all large waves are tracked while minor waves are neglected. Nonetheless, in all the experiments, as long as the thresholds do not suppress large waves, the drawn overall conclusions regarding wave

https://doi.org/10.5194/egusphere-2025-3867
Preprint. Discussion started: 15 August 2025

speed changes remain unchanged. We track each local ridge and trough in time over longitudes to find ridge and trough speed, respectively. Also, we save all local ridge positions (latitude and longitude: RPLL) and trough positions (TPLL). Note that the ridge and trough speeds as defined here are not the same as the phase or the group speed. Phase speed represents the speed of individual wave numbers, whereas the group velocity is the propagation of the wave «envelope». These are both different from the trough and ridge velocity of combined waves as investigated here. Consequently, here we will refer to the examined velocity simply as the wave speed or the speed of ridges and troughs, intentionally avoiding the terms phase speed or group speed.

2.4 Wave amplitude

To examine variations in the geopotential field's waviness, the meridional extent of a given isohypse (line of constant gph) is calculated by subtracting the maximum latitudinal location from the minimum location of each isohypse. However, due to the chaotic nature of the gph field, this method will, in some cases, lead to interpretation errors of the wave amplitude (see the supplementary information). We therefore refine the method to solve most of these interpretation ambiguities (see the supplementary information for a description of a refinement of the method and for examples of ambiguous gph fields). At a given pressure level, our developed metric provides the meridional extent of the Z1–5 ridges at the latitude and longitude location of its vertical extremes, RPLL. The meridional extent of the ridge is given as the latitudinal difference between the RPLL and the isohypse determined by the zonal average of the Z1–5 over a 90-degree longitude range centered at the RPLL (Fig. 1b and supplementary Fig. S3b). Hence, the meridional extent of a ridge at a given latitude is obtained as the difference between that latitude and the latitude of the first cross of the isohypse when moving northward at the longitude of the RPLL. The employed method does not take into account the possible meridional tilting of waves. To address this, the wave amplitude is calculated for all longitudes within the 90-degree longitude range. The highest value obtained is then considered the meridional amplitude of the ridge. While the highest value often yields slightly larger wave amplitudes than that at the RPLL, the overall conclusions regarding changes in wave amplitude during cold spells remain the same for both approaches (not shown). The meridional extent of troughs is obtained in a similar way but moving southward from TPLL.

The estimated value of wave amplitude is highly influenced by the longitudinal range over which the zonal average of the Z1–5 is taken for determining the isohypse. Using a smaller longitude range yields an isohypse value closer to the value of the gph at RPLL (TPLL). This can lead to small wave amplitude values. Using a large longitude range might yield an isohypse that cannot be found near the RPLL (TPLL), resulting in a missing value for the amplitude. Therefore, after conducting multiple experiments, the 90-degree threshold is chosen. Nonetheless, despite the arbitrariness of the meridional wave amplitude when defined this way, its magnitude remains consistent across latitudes and between climatology and cold spell cases, which is important and sufficient for this study.

2.5 Significant test

To test the null hypothesis that anomalies associated with the cold spells are zero, a Monte Carlo simulation with random samples is employed. Specifically, the average number of cold spell days across each region is compared with the average of

https://doi.org/10.5194/egusphere-2025-3867
Preprint. Discussion started: 15 August 2025

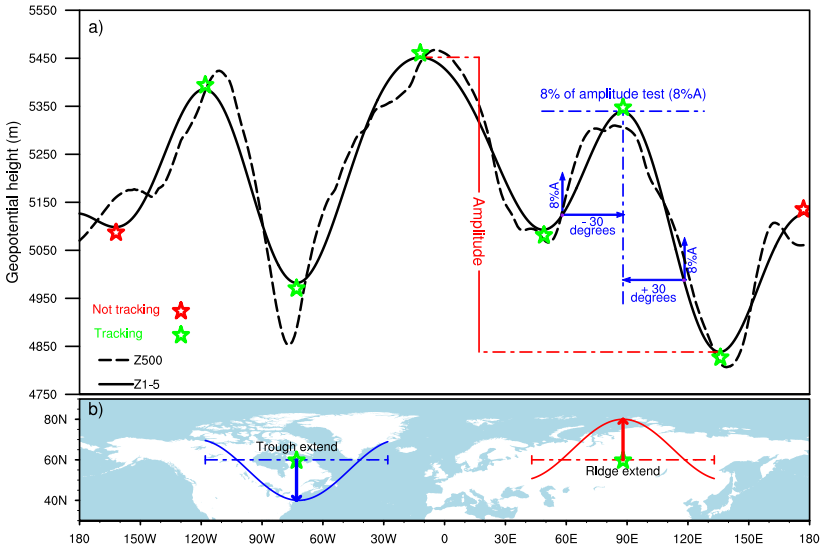

Figure 1. a) The 500 hPa geopotential height field (Z500; dashed, black line) and the sum of the first five zonal Fourier-decomposed waves of Z500 (Z1–5; solid, black line) for a randomly selected time step. The blue text and arrows are associated with a threshold metric that identifies the strength of the ridges and troughs (see method for more information). Based on this threshold, three ridges and three troughs (green stars) are high and deep enough, respectively, for being detected by the tracking algorithm. In this time step, the tracking algorithm will ignore one ridge and one trough (red stars) that do not meet this threshold. b) Schematic of ridge (red arrow) and trough (blue arrow) meridional amplitudes.

an equivalent number of randomly selected days. Instead of selecting random days from the entire winter season, the selection is weighted based on the frequency distribution through the season of cold spell days, since cold spells appear to occur more frequently in some parts of winter. This Monte Carlo test is repeated at least 2000 times to ensure a sufficient sample size, and significant differences from zero are identified at the 95% confidence level.

https://doi.org/10.5194/egusphere-2025-3867
Preprint. Discussion started: 15 August 2025

3 Results

3.1 Wave location

To investigate the impact of planetary waves on the formation of winter cold spells, nine regions with a high likelihood of cold spells are selected (Fig. 2). These regions are chosen based on their significant contribution to the historical extreme cold days on a hemispheric scale (see the supplementary information). In all the study regions, except Northern Siberia, cold days typically coincide with an upstream anticyclonic gph anomaly and a downstream cyclonic gph anomaly (supplementary Fig. S2). It has been demonstrated that northern hemisphere extratropic cold spells are generally established by northerly cold advection (Pfahl, 2014; Tuel and Martius, 2024), indicating that both cyclonic and anticyclonic gph anomalies play a role in transporting cold air masses from higher latitudes to areas developing and undergoing cold spells.

Fig. 2 displays the probability for the positions of ridges and troughs for winter climatology. Most often three major ridges and three major troughs can be seen throughout winters (Fig. 2 and supplementary Fig. S5). The three main ridges are located over the west coast of North America (hereafter, WNA ridge), the western flank of the Tibetan Plateau (hereafter, TP ridge), and the North Atlantic Ocean (hereafter, NAO ridge, at low latitude over the middle part, and at high latitude over the eastern part of the ocean). The three main troughs are located over Eastern North America (hereafter, ENA trough), the eastern Mediterranean (hereafter, EMed trough), and East Asia (hereafter, EAsia trough). The location of the WNA ridge, TP ridge, ENA trough, and EAsia trough are mainly determined by large mountain ranges, which force a westerly flow to ascend and move northward along their western slopes, creating a ridge, and descend and move southward on the leeward side, developing a trough (Bolin, 1950; Held, 2001). In addition, the intrinsic relationship between relative and planetary vorticity (that the potential vorticity is almost conserved) implies that mountains cause the zonal air stream to move meridionally and thereby initiate waves in the mid-latitudes (Holton and Hakim, 2013).

During cold spells, a distinct shifting pattern of ridges and troughs occurs over each region (see the supplementary information for details). Before the onset of cold spells (Fig. 3a, b), upstream ridges encompass a broad area, including the cold-spell region, while downstream troughs are located outside. At the start of cold spells, upstream ridges shift to be located outside of the cold-spell region, while downstream troughs are now found inside (Fig. 3c). This configuration enhances the northerly wind flow from the Arctic toward the cold-spell location, potentially advecting cold air into the region (see supplementary Fig. S6). These findings highlight the critical role of the nearest upstream ridge and downstream trough in the formation of cold spells.

3.2 Wave amplitude and speed

Several studies link the increased likelihood of cold temperature extremes in mid-latitudes to increased upper-atmosphere waviness (e.g., Fragkoulidis et al., 2018). Some studies link extreme cold temperatures to a significant amplified circumglobal waviness based on wave amplitudes of individual wave numbers (Petoukhov et al., 2013; Screen and Simmonds, 2014), while others assert a robust correlation between local waviness and cold temperature extremes (Röthlisberger et al., 2016; Fragkoulidis et al., 2018). Local waviness metrics, such as the Rossby wave packet amplitude, combine the ridge and trough into a

https://doi.org/10.5194/egusphere-2025-3867
Preprint. Discussion started: 15 August 2025

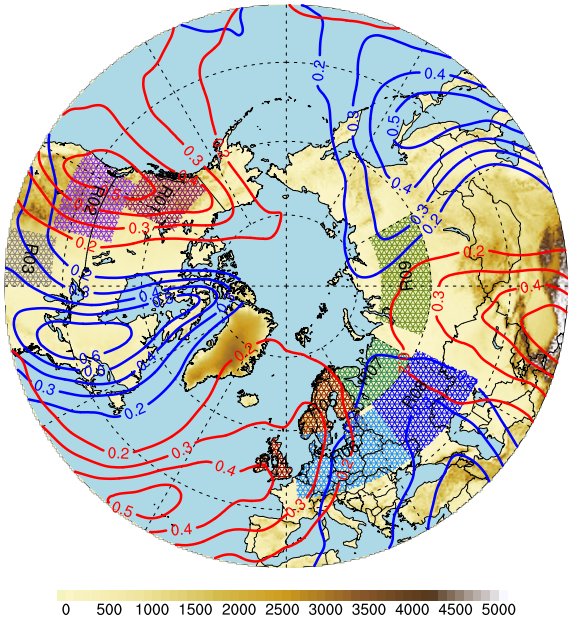

Figure 2. The probability (in percentage) of the position of 300 hPa ridges (red contours) and troughs (blue contours) during winter climatology. The contours indicate probabilities of vertical extremes in latitude and longitude. The hatches indicate the chosen regions for the study on cold spells. A Gaussian function, using a weighted running average over eight degrees in latitude and over an equal distance in longitude, is used to smooth the probabilities. Shading shows the elevation above mean sea level (m).

single unit; therefore, it is unclear how these wave features individually contribute to the amplitude. Previous studies have also shown that the speed of atmospheric waves significantly contributes to cold extreme temperatures in mid-latitudes (e.g., Jolly et al., 2021; van Mourik et al., 2025). Slower wave phase speed has been linked to more persistent weather in which extreme cold temperatures can develop, such as atmospheric blocking (Riboldi et al., 2020). However, these studies do not establish the
165 role of each ridge and trough in cold spells, and further research is needed to understand how individual wave features interact to influence temperature extremes. Here, we aim to explore the linkage between cold spells and the amplitude and speed of each ridge and trough (see the supplementary and the method sections for details).

Given the location of ridges and troughs at 300 hPa (Fig. 2) and 500 hPa (supplementary Fig. S5), the longitudinal average of the wave amplitudes and speeds for the climatology and cold spells is calculated in three longitude bands: the amplitudes

https://doi.org/10.5194/egusphere-2025-3867
Preprint. Discussion started: 15 August 2025

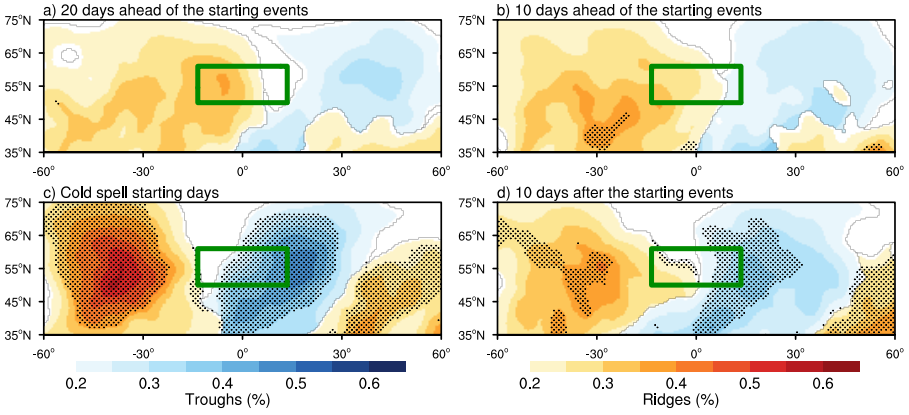

Figure 3. The probability (in percentage) of the position of 300 hPa ridges (red shading) and troughs (blue shading) for different time lags averaged over all cold spells and all study regions relative to the center of the cold-spell region. The shading indicates probabilities of vertical extremes in latitude and longitude. As the probabilities of ridges and troughs are computed individually, shading of the two fields are shown for values greater than 0.2% to minimize overlap in the plot. Dots indicate regions where cold spells and climatology are significantly different at the 95% confidence level. The green box shows the average latitude and longitude span of all cold spell regions. A Gaussian function, using a weighted running average over eight degrees in latitude and over an equal distance in longitude, is used to smooth the probabilities. a) 20 days ahead of the starting cold spells, b) 10 days ahead of the starting cold spells, c) cold spell starting days, and d) 10 days after the start of cold spells.

and speeds of the ridges over 180°W–90°W, 60°W–30°E, and 30°E–120°E are averaged to calculate the amplitudes and speeds of the WNA ridge, the NAO ridge, and the TP ridge, respectively. The amplitudes and speeds of the ENA trough, EMed trough, and EAsia trough are also found by taking the average of the amplitudes and speeds of the troughs over 120°W–30°W, 0°E–90°E, and 90°E–150°W, respectively.

https://doi.org/10.5194/egusphere-2025-3867
Preprint. Discussion started: 15 August 2025

For cold spells, the largest ridge and trough amplitude and speed differences relative to climatology occur for the local upstream ridge and downstream trough (supplementary Figs. S7 and S8). Generally, the amplitude and speed differences of ridges and troughs decay as their distance increases to the location of the cold spell. A composite over all cold spells and regions of the upstream ridges and downstream troughs provides a general overview of the local wave behavior during cold spells (Fig. 4). The upstream ridge significantly amplifies (Fig. 4a and supplementary Fig. S7), facilitating the transfer of Arctic cold air to the cold spell region. The amplification of this ridge also implies the development of higher gph values (warmer air) at higher latitudes, as is also evident in the supplementary Fig. S2. During cold spells, the northward winds entering the Arctic are increasing west of the upstream ridge, while the southward winds exiting the Arctic are increasing east of the upstream ridge (supplementary Fig. S6). The upstream ridge also significantly slows down (Fig. 4b and supplementary Fig. S8), implying the persistence of the warm northward wind to the Arctic and the cold southward wind to the cold spell location. The persistent warm northward wind to the Arctic might be the reason behind the correlation between cold events and a warmer Arctic found in the other studies (e.g., Cohen et al., 2018); yet more research is needed to discover the impact of the amplified ridge on Arctic temperatures.

The downstream trough amplifies (deepens) at latitudes north of the cold spell location, while it weakens at southerly latitudes (Fig. 4a and supplementary Fig. S7). For the cold-spell regions in the southern as compared to the northern mid-latitudes, the increase in trough amplitude develops more to the south (supplementary Fig. S7). Amplification of this trough contributes to enhancing the southward cold wind from the Arctic into the cold spell region (supplementary Fig. S6). Similar to the upstream ridge, the downstream trough significantly slows down (Fig. 4b and supplementary Fig. S8), hereby increasing the persistency of the cold southward winds into the cold spell region.

3.3 Causality

In the previous section, we have shown that cold spells are associated with higher-amplitude and slowing ridges and troughs in the vicinity of the cold spells. The question that arises is whether cold spells cause the amplification and slowdown of waves or vice versa. Previous research has shown that upper-atmospheric changes—such as amplified planetary waves (Screen and Simmonds, 2014) , blocking (Kautz et al., 2022), and the stratospheric polar vortex (Tomassini et al., 2012)—can lead to surface extreme events. Nevertheless, the mechanism by which upper-level changes favor extreme surface weather is not clear. Here, a day-lag analysis of composites over cold spells is provided to shed light on the causal relationship between upper-level waves and surface temperature (Fig. 5 and supplementary Fig. S9). Since the largest wave amplitude and speed differences relative to climatology belong to the upstream ridge and the downstream trough, their time series are plotted here.

The minimum speeds of the upstream ridge and downstream trough occur at a negative time lag several days prior to the onset of the cold spell, which is taken as 30 percent of grid points in the region experiencing a cold spell and indicated by the lag zero. The wave speed anomaly shows almost a similar pattern for both 500 hPa and 300 hPa (Fig. 5a and b). This pattern suggests an almost barotropic wave signal through the troposphere during cold spell events. However, the wave-speed reduction occurs somewhat later at 850 hPa, indicating a downward propagation of the wave-speed signal.

https://doi.org/10.5194/egusphere-2025-3867
Preprint. Discussion started: 15 August 2025

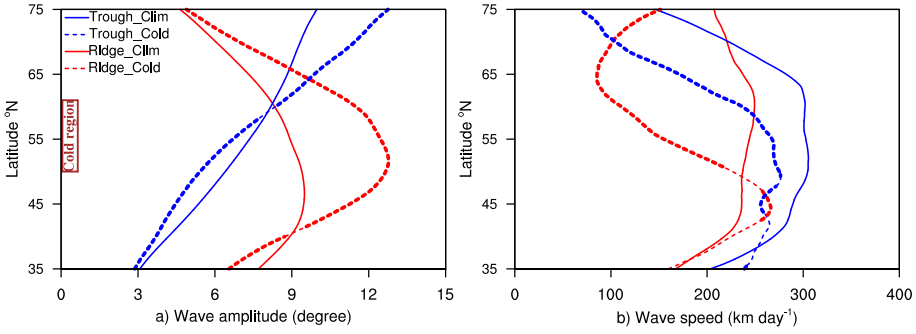

Figure 4. Climatology (solid lines) and composite of cold spells over all study regions (dashed lines) for a) wave amplitude (degree) and b) wave speed ($\mathrm{km\,day^{-1}}$) at 300 hPa. Red and blue lines are showing the average of the upstream ridge and the downstream trough, respectively, in the vicinity of each cold spell region. Bold dashed lines indicate difference between cold spell and climatology at the 95% confidence level. The brown box on the left side shows the average latitude span of all regions. A four-degree running average is used to smooth the lines.

Both amplified ridge and trough are also encountered prior to the cold spell, but the speed reduction precedes the amplitude increase (Fig. 5a and b). This could potentially be attributed to the breaking of waves due to exceeding the capacity of the wave for the wave activity flux (Nakamura and Huang, 2018). The preceding of the upstream ridge and the downstream trough amplification relative to the cold spell suggests that cold spells arise as a result of slow and amplified local upper-atmospheric waves.

The upstream ridge maximizes simultaneously at all three levels, while the downstream trough amplifies almost simultaneously at 500 and 300 hPa and one day later at 850 hPa. This indicates that during cold spells, the upstream ridge amplification is barotropic, whereas in the lower troposphere, the downstream trough amplification is somewhat baroclinic. It has been shown that during cold spells over China, the positive gph anomaly has a barotropic structure and the negative gph anomaly has a baroclinic structure in the lower troposphere (Zhang et al., 2021).

There is no indication that the upstream ridge anomaly is encountered prior to the downstream trough anomaly or vice versa. This suggests that the anomalies could emerge independently in both the ridge and the trough. For instance, in January 2014,

https://doi.org/10.5194/egusphere-2025-3867
Preprint. Discussion started: 15 August 2025

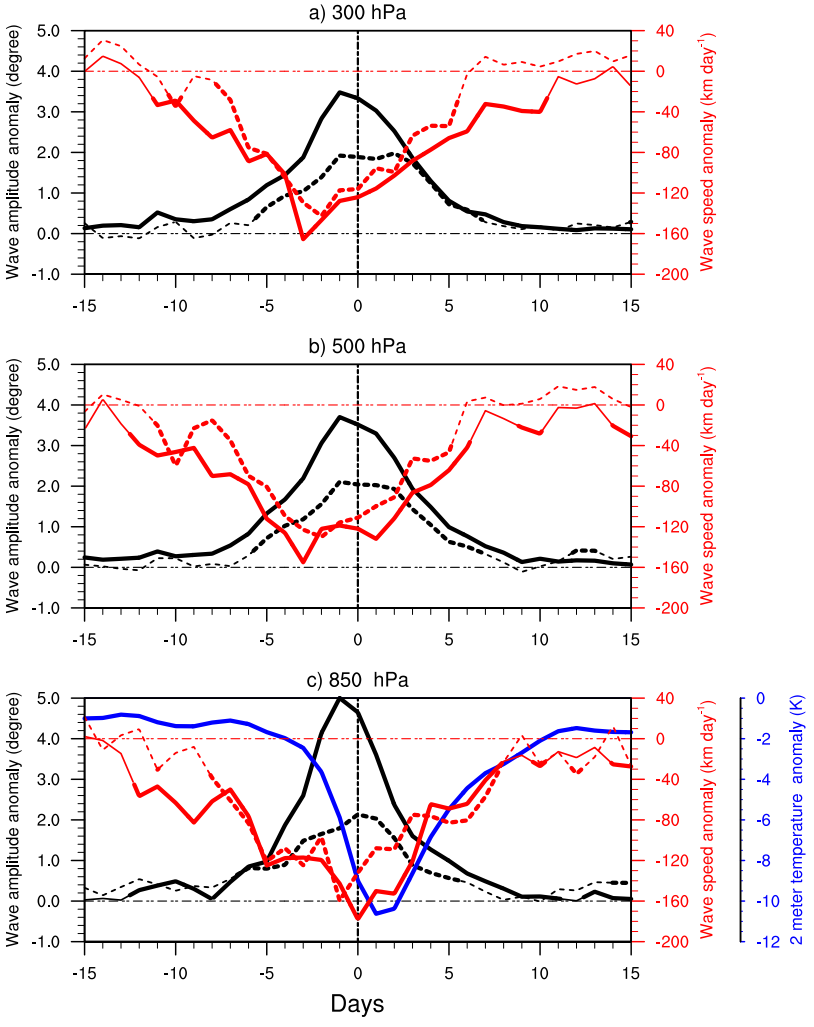

Figure 5. Composites of anomalies relative to climatology of 2-meter temperature, and ridge and trough speed and amplitude during all cold spells as a function of time lag for all study regions. The lag zero (zero on the x-axis) is the day that 30% of the land in each region experiences a cold spell. Blue line is the composite of temperature anomalies averaged over the whole study region. Black and red lines are the composites of ridge and trough amplitude and speed anomalies, respectively. The upstream ridge and the downstream trough in the vicinity of the cold-spell location are shown by solid and dashed lines, respectively. The latitude bands with a significant positive wave amplitude anomaly and a negative wave speed anomaly are averaged for each cold spell region (indicated by the vertical solid lines on the right side of the supplementary Figs. S7 and S8). Bolded solid and bolded dashed lines indicate the difference to climatology significant on a 95% level. a) 300 hPa, b) 500 hPa, and c) 850 hPa.

poleward low potential vorticity from subtropical deep convection amplified the WNA ridge, while equatorward and downward high potential vorticity deepened the ENA trough (Davies, 2015). Li et al. (2017) also showed that only the breakdown of the

https://doi.org/10.5194/egusphere-2025-3867
Preprint. Discussion started: 15 August 2025

stratospheric polar vortex cannot be a reliable predictor of cold spells in North America, and warm sea surface temperature in the eastern extratropical Pacific also needs to be considered.

4 Conclusions

The present study provides a large-scale perspective of changes in Rossby waves during cold spells. Here we show that locally amplified and slowing Rossby waves in the vicinity of cold spells are favoring the advection of Arctic cold air into the cold-spell region. Our findings support previous research indicating that slow (e.g., Fragkoulidis et al., 2018) and amplified (e.g., Jolly et al., 2021) Rossby waves contribute to cold spells in mid-latitudes. Additionally, we discuss the importance of wave location in cold spell development, as shifting the location of waves relative to climatology can result in a cold air advection to the cold region. Our findings highlight the critical importance of wave location, emphasizing the need to consider potential shifts in wave positions in a warming world. Such shifts could result in more frequent extreme events in certain areas, impacting local climates.

Considering the increasing frequency of heat waves, floods, and droughts due to climate change (IPCC; Seneviratne et al., 2021), there is a need to understand the dynamical drivers of them (Xu et al., 2024). In this context, we have developed two tools designed to identify the amplitude and speed of atmospheric waves, which can be utilized in future research to unravel the dynamical drivers of various extreme events. Furthermore, these metrics may help clarify the impact of AA on the waviness and speed of Rossby waves. Our meridional wave amplitude metric provides a unique methodology compared to other metrics, as it could evaluate changes in ridge and trough independently in a warming world.

Code availability. Codes are available at https://doi.org/10.5281/zenodo.16761350

Data availability. We obtained the ERA5 data from the ECMWF data server on pressure levels at https://cds.climate.copernicus.eu/datasets/reanalysis-era5-pressure-levels?tab=download and single levels at https://cds.climate.copernicus.eu/datasets/reanalysis-era5-single-levels?tab=download.

Author contributions. All authors conceived and designed the study. Material preparation, data collection and analysis were performed by MB. The first draft of the manuscript was written by MB with comments and revisions from RGG and JPS.

Competing interests. The authors declare no competing interests.

https://doi.org/10.5194/egusphere-2025-3867
Preprint. Discussion started: 15 August 2025

Acknowledgements. The work is part of the project: The role of atmospheric circulation in extreme weather events, funded by the Faculty of Science and Technology, University of Tromsø.

https://doi.org/10.5194/egusphere-2025-3867
Preprint. Discussion started: 15 August 2025

References

Barnes, E. A.: Revisiting the evidence linking Arctic amplification to extreme weather in midlatitudes, Geophys. Res. Lett., 40, 4734–4739, https://doi.org/https://doi.org/10.1002/grl.50880, 2013.

Berggren, R., Bolin, B., and Rossby, C. G.: An Aerological Study of Zonal Motion, its Perturbations and Break-down, Tellus, 1, 14–37, https://doi.org/https://doi.org/10.1111/j.2153-3490.1949.tb01257.x, 1949.

Bjerknes, J.: Theorie der aussertropischen Zyclonenbildung, Meteor. Zeit., 54, 462–466, 1937.

Blackport, R., Fyfe, J. C., and Screen, J. A.: Arctic change reduces risk of cold extremes, Science, 375, 729–729, https://doi.org/10.1126/science.abn2414, 2022.

Blackport, R., Sigmond, M., and Screen, J. A.: Models and observations agree on fewer and milder midlatitude cold extremes even over recent decades of rapid Arctic warming, Sci. Adv., 10, eadp1346, https://doi.org/10.1126/sciadv.adp1346, 2024.

Bolin, B.: On the Influence of the Earth's Orography on the General Character of the Westerlies, Tellus, 2, 184–195, https://doi.org/10.3402/tellusa.v2i3.8547, 1950.

Cassidy, E.: Arctic chill sweeps U.S., https://earthobservatory.nasa.gov/images/152333/arctic-chill-sweeps-us, 2024.

Cohen, J., Screen, J. A., Furtado, J. C., Barlow, M., Whittleston, D., Coumou, D., and Jones, J.: Recent Arctic amplification and extreme mid-latitude weather, Nat. Geosci., 7, 627–637, https://doi.org/https://doi.org/10.1038/ngeo2234, 2014.

Cohen, J., Pfeiffer, K., and Francis, J. A.: Warm Arctic episodes linked with increased frequency of extreme winter weather in the United States, Nat. Commun., 9, 869, https://doi.org/https://doi.org/10.1038/s41467-018-02992-9, 2018.

Cohen, J., Agel, L., Barlow, M., Garfinkel, C. I., and White, I.: Linking Arctic variability and change with extreme winter weather in the United States, Science, 373, 1116–1121, https://doi.org/10.1126/science.abi9167, 2021.

Cohen, J., Francis, J. A., and Pfeiffer, K.: Anomalous Arctic warming linked with severe winter weather in Northern Hemisphere continents, Commun. Earth Environ., 5, 557, https://doi.org/https://doi.org/10.1038/s43247-024-01720-0, 2024.

Coumou, D., Lehmann, J., and Beckmann, J.: The weakening summer circulation in the Northern Hemisphere mid-latitudes, Science, 348, 324–327, https://doi.org/10.1126/science.1261768, 2015.

Davies, H. C.: Weather chains during the 2013/2014 winter and their significance for seasonal prediction, Nat. Geosci., 8, 833–837, https://doi.org/https://doi.org/10.1038/ngeo2561, 2015.

Doermann, L.: Extreme Nordic cold, https://earthobservatory.nasa.gov/images/152288/extreme-nordic-cold, 2024.

Fischer, E. M., Sippel, S., and Knutti, R.: Increasing probability of record-shattering climate extremes, Nat. Clim. Chang., 11, 689–695, https://doi.org/https://doi.org/10.1038/s41558-021-01092-9, 2021.

Fragkoulidis, G., Wirth, V., Bossmann, P., and Fink, A. H.: Linking Northern Hemisphere temperature extremes to Rossby wave packets, Q. J. R. Meteorol. Soc., 144, 553–566, https://doi.org/https://doi.org/10.1002/qj.3228, 2018.

Francis, J. A. and Vavrus, S. J.: Evidence linking Arctic amplification to extreme weather in mid-latitudes, Geophys. Res. Lett., 39, 2012GL051 000, https://doi.org/https://doi.org/10.1029/2012GL051000, 2012.

Held, I. M.: Stationary and quasi-stationary eddies in the extratropical troposphere: theory, in: Large-scale Dynamical Processes in the Atmosphere, edited by Hoskins, B. and Pearce, R., pp. 127–168, Academic Press, New York, 2001.

Hersbach, H., Bell, B., Berrisford, P., Hirahara, S., Horányi, A., Muñoz-Sabater, J., Nicolas, J., Peubey, C., Radu, R., Schepers, D., Simmons, A., Soci, C., Abdalla, S., Abellan, X., Balsamo, G., Bechtold, P., Biavati, G., Bidlot, J., Bonavita, M., De Chiara, G., Dahlgren, P., Dee, D., Diamantakis, M., Dragani, R., Flemming, J., Forbes, R., Fuentes, M., Geer, A., Haimberger, L., Healy, S., Hogan, R. J., Hólm, E.,

https://doi.org/10.5194/egusphere-2025-3867
Preprint. Discussion started: 15 August 2025

Janisková, M., Keeley, S., Laloyaux, P., Lopez, P., Lupu, C., Radnoti, G., de Rosnay, P., Rozum, I., Vamborg, F., Villaume, S., and Thépaut, J.-N.: The ERA5 global reanalysis, Q. J. R. Meteorol. Soc., 146, 1999–2049, https://doi.org/https://doi.org/10.1002/qj.3803, 2020.

Holton, J. R. and Hakim, G. J.: An introduction to dynamic meteorology, Academic Press, https://doi.org/https://doi.org/10.1016/C2009-0-63394-8, 2013.

Hoskins, B. and Woollings, T.: Persistent Extratropical Regimes and Climate Extremes, Curr. Climate Change Rep., 1, 115–124, https://doi.org/https://doi.org/10.1007/s40641-015-0020-8, 2015.

Iturbide, M., Gutiérrez, J. M., Alves, L. M., Bedia, J., Cerezo-Mota, R., Cimadevilla, E., Cofiño, A. S., Di Luca, A., Faria, S. H., Gorodetskaya, I. V., Hauser, M., Herrera, S., Hennessy, K., Hewitt, H. T., Jones, R. G., Krakovska, S., Manzanas, R., Martínez-Castro, D., Narisma, G. T., Nurhati, I. S., Pinto, I., Seneviratne, S. I., van den Hurk, B., and Vera, C. S.: An update of IPCC climate reference regions for subcontinental analysis of climate model data: definition and aggregated datasets, Earth Syst. Sci. Data, 12, 2959–2970, https://doi.org/10.5194/essd-12-2959-2020, 2020.

Jolly, E., d'Andrea, F., Rivière, G., and Fromang, S.: Linking warm Arctic winters, Rossby waves, and cold spells: an idealized numerical study, J. Atmos. Sci., 78, 2783–2799, https://doi.org/https://doi.org/10.1175/JAS-D-20-0088.1, 2021.

Kautz, L. A., Martius, O., Pfahl, S., Pinto, J. G., Ramos, A. M., Sousa, P. M., and Woollings, T.: Atmospheric blocking and weather extremes over the Euro-Atlantic sector–a review, WCD, 3, 305–336, https://doi.org/10.5194/wcd-3-305-2022, 2022.

Li, Z., Manson, A. H., Li, Y., and Meek, C.: Circulation characteristics of persistent cold spells in central–eastern North America, J. Meteorol. Res., 31, 250–260, https://doi.org/https://doi.org/10.1007/s13351-017-6146-y, 2017.

Macdonald, N. J.: On the apparent relationship between convective activity and the shape of 500 mb troughs, Mon. Wea Rev., 104, 1618–1622, https://doi.org/10.1175/1520-0493(1976)104<1618:OTARBC>2.0.CO;2, 1976.

Morlot, M., Russo, S., Feyen, L., and Formetta, G.: Trends in heat and cold wave risks for the Italian Trentino-Alto Adige region from 1980 to 2018, NHESS, 23, 2593–2606, 2023.

Nakamura, N. and Huang, C. S.: Atmospheric blocking as a traffic jam in the jet stream, Science, 361, 42–47, https://doi.org/10.1126/science.aat0721, 2018.

Namias, J. and Clapp, P. F.: STUDIES OF THE MOTION AND DEVELOPMENT OF LONG WAVES IN THE WESTERLIES, J. Atmos. Sci, 1, 57–77, https://doi.org/10.1175/1520-0469(1944)001<0057:SOTMAD>2.0.CO;2",, 1944.

NOAA: U.S. had its warmest winter on record, https://www.noaa.gov/news/us-had-its-warmest-winter-on-record, 2024.

NOAA: U.S. Billion-Dollar Weather and Climate Disasters, https://doi.org/10.25921/stkw-7w73, 2025.

Overland, J. E., Ballinger, T. J., Cohen, J., Francis, J. A., Hanna, E., Jaiser, R., Kim, B. M., Kim, S. J., Ukita, J., Vihma, T., Wang, M., and Zhang, X.: How do intermittency and simultaneous processes obfuscate the Arctic influence on midlatitude winter extreme weather events?, Environ. Res. Lett., 16, 043 002, https://doi.org/10.1088/1748-9326/abdb5d, 2021.

Petoukhov, V., Rahmstorf, S., Petri, S., and Schellnhuber, H. J.: Quasiresonant amplification of planetary waves and recent Northern Hemisphere weather extremes, Proc. Natl. Acad. Sci. U.S.A., 110, 5336–5341, https://doi.org/10.1073/pnas.1222000110, 2013.

Pfahl, S.: Characterising the relationship between weather extremes in Europe and synoptic circulation features, NHESS, 14, 1461–1475, https://doi.org/10.5194/nhess-14-1461-2014, 2014.

Pfleiderer, P. and Coumou, D.: Quantification of temperature persistence over the Northern Hemisphere land-area, Clim. Dyn., 51, 627–637, https://doi.org/https://doi.org/10.1007/s00382-017-3945-x, 2018.

Riboldi, J., Lott, F., D'Andrea, F., and Rivière, G.: On the Linkage Between Rossby Wave Phase Speed, Atmospheric Blocking, and Arctic Amplification, Geophys. Res. Lett., 47, e2020GL087 796, https://doi.org/https://doi.org/10.1029/2020GL087796, 2020.

https://doi.org/10.5194/egusphere-2025-3867
Preprint. Discussion started: 15 August 2025

Rossby, C. G., Willett, H. C., Holmboe, M., Namias, J., Page, L., and Allen, R.: Relation between variations in the intensity of the zonal circulation of the atmosphere and the displacements of the permanent centers of action, J. Mar. Res., 1939.

Röthlisberger, M., Pfahl, S., and Martius, O.: Regional-scale jet waviness modulates the occurrence of midlatitude weather extremes, Geophys. Res. Lett., 43, 10,989–10,997, https://doi.org/https://doi.org/10.1002/2016GL070944, 2016.

Screen, J. A. and Simmonds, I.: Exploring links between Arctic amplification and mid-latitude weather, Geophys. Res. Lett., 40, 959–964, https://doi.org/https://doi.org/10.1002/grl.50174, 2013.

Screen, J. A. and Simmonds, I.: Amplified mid-latitude planetary waves favour particular regional weather extremes, Nat. Clim. Chang., 4, 704–709, https://doi.org/https://doi.org/10.1038/nclimate2271, 2014.

Seneviratne, S. I., Zhang, X., Adnan, M., Badi, W., Dereczynski, C., Luca, A. D., Ghosh, S., Iskandar, I., Kossin, J., Lewis, S., Otto, F., Pinto, I., Satoh, M., Vicente-Serrano, S. M., Wehner, M., Zhou, B., and Allan, R.: Weather and climate extreme events in a changing climate, in: Climate Change 2021: The Physical Science Basis: Working Group I contribution to the Sixth Assessment Report of the Intergovernmental Panel on Climate Change, edited by Masson-Delmotte, V. P., Zhai, A., Pirani, S. L., and Connors, C., pp. 1513–1766, Cambridge University Press, Cambridge, UK, https://doi.org/10.1017/9781009157896.013, 2021.

Stendel, M., Francis, J., White, R., Williams, P. D., and Woollings, T.: Chapter 15 - The jet stream and climate change, in: Climate Change (Third Edition), edited by Letcher, T. M., pp. 327–357, Elsevier, third edition edn., https://doi.org/https://doi.org/10.1016/B978-0-12-821575-3.00015-3, 2021.

Suardy, D. O.: Flash floods in Spain: Joining forces for rapid recovery, https://civil-protection-humanitarian-aid.ec.europa.eu/news-stories/stories/flash-floods-spain-joining-forces-rapid-recovery_en#:~:text=In%20late%20October%202024%2C%20a,their%20lives%2C%2013%20remain%20missing., 2024.

Tomassini, L., Gerber, E. P., Baldwin, M. P., Bunzel, F., and Giorgetta, M.: The role of stratosphere-troposphere coupling in the occurrence of extreme winter cold spells over northern Europe, J. Adv. Model. Earth Syst., 4, https://doi.org/https://doi.org/10.1029/2012MS000177, 2012.

Tuel, A. and Martius, O.: Persistent warm and cold spells in the Northern Hemisphere extratropics: regionalisation, synoptic-scale dynamics and temperature budget, WCD, 5, 263–292, https://doi.org/10.5194/wcd-5-263-2024, 2024.

van Mourik, J., de Vries, H., and Baatsen, M.: On the movement of atmospheric blocking systems and the associated temperature responses, WCD, 6, 413–429, https://doi.org/10.5194/wcd-6-413-2025, 2025.

White, R. H. and Mareshet, A., L.: Temporally and zonally varying atmospheric waveguides – climatologies and connections to quasi-stationary waves, WCD, pp. 549–570, https://doi.org/10.5194/wcd-6-549-2025, 2025.

White, R. H., Kornhuber, K., Martius, O., and Wirth, V.: From Atmospheric Waves to Heatwaves: A Waveguide Perspective for Understanding and Predicting Concurrent, Persistent, and Extreme Extratropical Weather, Bull. Am. Meteorol. Soc., 103, E923–E935, https://doi.org/10.1175/BAMS-D-21-0170.1, 2022.

Wicker, W., Harnik, N., Pyrina, M., and Domeisen, D. I.: Heatwave location changes in relation to Rossby wave phase speed, Geophys. Res. Lett., 51, e2024GL108 159, https://doi.org/https://doi.org/10.1029/2024GL108159, 2024.

WMO: Devastating rainfall hits Spain: Yet another flood-related disaster, https://wmo.int/media/news/devastating-rainfall-hits-spain-yet-another-flood-related-disaster, 2024.

Xu, G., Broadman, E., Dorado-Liñán, I., Klippel, L., Meko, M., Büntgen, U., De Mil, T., Esper, J., Gunnarson, B., Hartl, C., Krusic, P. J., Linderholm, H. W., Ljungqvist, F. C., Ludlow, F., Panayotov, M., Seim, A., Wilson, R., Zamora-Reyes, D., and Trouet, V.: Jet stream controls on European climate and agriculture since 1300 CE, Nature, 634, 600–608, https://doi.org/10.1038/s41586-024-07985-x, 2024.

https://doi.org/10.5194/egusphere-2025-3867
Preprint. Discussion started: 15 August 2025

Zhang, L., Xie, Z., Deng, Y., and Huang, W.: Structure and Large-Scale Organization of Extreme Cold Wave Events Over the Chinese Mainland During the Boreal Cold Season, J. Geophys. Res. Atmos., 126, e2021JD035 005, https://doi.org/10.1029/2021JD035005, 2021.

Zschenderlein, P., Fragkoulidis, G., Fink, A. H., and Wirth, V.: Large-scale Rossby wave and synoptic-scale dynamic analyses of the unusually late 2016 heatwave over Europe, Weather, 73, 275–283, https://doi.org/https://doi.org/10.1002/wea.3278, 2018.